Journal of Inflammation

RESEARCH Open Access

Divergence in photoreceptor cell death and neuroinflammation in transvitreal and transscleral subretinal delivery in mice

Daniel E. Maidana[1,2,3], Sara Pastor Puente[1], Catherine Wang[1], Shivam Chandra[1], Lucia Gonzalez-Buendia[3,4], Eleftherios Paschalis Ilios[3,5], Andrius Kazlauskas[1,2] and Demetrios G. Vavvas[3,5*]

Abstract

Subretinal injections provide direct access to photoreceptors and RPE, which is crucial for the delivery of gene therapy and neuroprotective approaches. To access the subretinal space, transvitreal (TV) and transscleral (TS) subretinal injections have been widely used in humans and animal models. In this work, we investigated recent trends and outcomes of utilizing TV and TS subretinal models of retinal detachment (RD). A literature review revealed an increasing utilization of both models over the past two decades, with TS emerging as the predominant model since 2012. Subretinal injection in CX3CR1 + /GFP CCR2 + /RFP mice revealed early inflammatory responses, with TS injections inducing higher infiltration of CD11b + CCR2 + cells compared to TV. Further leukocyte immunophenotyping indicated divergent infiltration patterns, with the TS approach exhibiting higher proportions of neutrophils and macrophages/microglia-like cells, while the TV injections had higher CD45hi CD11b + Ly6G- Ly6C + infiltration. Notably, late-stage analysis demonstrates higher photoreceptor cell death in the TS approach, paralleled by increased subretinal infiltration of CD11b + cells. Both models showed significant reactive gliosis, suggesting comparable late-stage wound healing responses. These findings underscore the utility of these approaches for subretinal delivery, offering insights into their distinctive leukocyte infiltration and late-stage tissue responses.

Keywords Retinal detachment, Outer nuclear layer, CD11b, CX3CR1, CCR2, Gliosis, Monocytes, Gene therapy

Introduction

The subretinal space (SRS) is a virtual space between the neurosensory retina and retinal pigment epithelium (RPE), which provides direct access to photoreceptors and other retina neurons. For this reason, the subretinal injection of genetic vectors and cellular therapies for these cells has been instrumental in delivering neuroprotective and regenerative approaches for retinal degeneration. To access the SRS, different subretinal injection approaches have been described to deliver such agents. In rodent preclinical studies, the most widely used methods to access the subretinal space are: i) transvitreal (TV) or *ab interno*, accessing the eye through an external sclerotomy, though the choroid, RPE, retina, vitreous cavity posterior to the lens, and tapping into the retina from the inner limiting membrane to the subretinal space [1, 2]; and ii) transscleral (TS) or *ab externo*, via an external sclerotomy, penetrating through the sclera, choroid, and RPE, ultimately reaching the subretinal space, without

*Correspondence:
Demetrios G. Vavvas
Demetrios_Vavvas@MEEI.HARVARD.EDU
[1] Department of Ophthalmology and Visual Sciences, Illinois Eye and Ear Infirmary, University of Illinois at Chicago, Chicago, IL, USA
[2] Department of Physiology and Biophysics, University of Illinois at Chicago, Chicago, IL, USA
[3] Retina Service, Angiogenesis Lab, Massachusetts Eye and Ear Infirmary, Harvard Medical School, Boston, MA, USA
[4] Institute of Ocular Microsurgery (IMO) Miranza Group, Madrid, Spain
[5] Massachusetts Eye and Ear Infirmary, 243 Charles Street, Boston, MA 02114, USA

creating a retinotomy [3]. Additionally, the suprachoroidal space can also be accessed using this approach.

Subretinal injections provide straightforward access to photoreceptors and RPE at the expense of a local retinal detachment (RD). Chorioretinal atrophy following subretinal gene therapy delivery has been described within and outside the injection site [4]. Moreover, injection of small volumes (100 µL) to the SRS in nonhuman primates has shown early electrophysiological suppression and late ultrastructural retinal changes [5]. The response of the host retina to these injections has been extensively studied using experimental models of RD, which provide invaluable insights into the kinetics of photoreceptor cell death [6–10]. Moreover, these models have been instrumental in unveiling the neuroinflammatory mechanisms associated with the detachment of the neurosensory retina by subretinal injection, identifying critical cellular and humoral mediators in this process [11–16]. Although technically challenging, experimental RD models are crucial to tailoring neuroprotective and regenerative therapeutic approaches, including drug and gene therapy delivery [17]. However, given the different structures involved while accessing the SRS via TV or TS injections, the impact of these different approaches on immune-mediated photoreceptor damage of the host retina remains unknown.

In this work, we investigated the early and late cellular events associated with an induced retinal detachment via TV and TS subretinal injections, particularly photoreceptor cell death, leukocyte infiltration, and retinal gliosis. We observed significant differences in photoreceptor cell death and divergence in leukocyte subtype infiltration of the retina across these injection types. These results suggest that given its different burden on the host retina, the injection route is a relevant factor in subretinal drug delivery. The appropriate selection of these routes can ultimately affect the clinical applicability of therapeutic strategies for retinal degenerative diseases.

Materials and Methods

All reagents used in this work are listed in Supplementary Table 1 with their respective manufacturer and catalog number.

Animals and Breeding

The animals used for experiments and breeding strictly followed the guidelines set forth by the Association for Research in Vision and Ophthalmology (ARVO). The Animal Care Committee of the University of Illinois Chicago reviewed and approved all animal protocols. The C57BL/6 J and CX3CR1$^{+/GFP}$ CCR2$^{+/RFP}$ strains were procured from The Jackson Laboratories. Nrl-EGFP^{+} mice were kindly provided by Anand Swaroop, Ph.D. (National Eye Institute, Bethesda, MD). Eight-week-old male and female mice were used for experiments. Animals were maintained in a standard 12-h light/dark cycle and provided ad libitum access to standard chow. Mice were randomly assigned to experimental groups.

Retinal Detachment Model

Animals were anesthetized with ketamine (80 mg/kg) and xylazine (5 mg/kg) via intraperitoneal injection. Pupils were dilated with phenylephrine 2.5% and tropicamide 1% drops. Proparacaine hydrochloride 0.5% was instilled to provide topical anesthesia. All retinal detachments were performed by a single investigator (DEM).

The TV retinal detachment model was performed as previously described [1, 2]. Briefly, a sclerotomy was performed in the nasal sclera, and a 34-gauge injector was inserted through the sclera/choroid, RPE, nasal retina, and vitreous cavity posterior to the lens. Under direct visualization, the tip of the injector was placed on the retinal surface and tapped into the subretinal space. A total of 4 µL of 1% sodium hyaluronate (Provisc, Alcon) was injected into the subretinal space to detach the temporal retina. The injector was removed with caution from the eye to avoid lens contact.

The TS model was performed as described by Matsumoto et al. [3] Briefly, a sclerotomy was performed in the temporal sclera, and a corneal paracentesis was performed. A 34-gauge injector was inserted through the sclera/choroid and RPE. Four µL of 1% sodium hyaluronate were injected into the subretinal space to detach the temporal retina. The injector was removed slowly to avoid leakage. The sclerotomy was sealed with cyanoacrylate-based surgical adhesive (Vetbond®, 3 M).

Following RD, Bacitracin ointment was placed in the eye. Eyes with cataracts, leakage, vitreous, retinal, or subretinal hemorrhage were excluded from further analysis.

Immunofluorescence

Eyes were harvested and fixed in 4% paraformaldehyde solution. Samples were embedded in Tissue-Tek® optimal cutting temperature compound (Sakura Finetek USA, CA). Eyecups were dissected, and the retina was isolated for wholemount analysis. Primary antibodies were incubated overnight at 4°C, while secondary antibodies were incubated for 2 h at room temperature. Whole eyes were processed to 10 µm axial cryosections, starting at 800 µm from the eye, and stored at −80°C. Slides were counterstained with 4',6-diamidino-2-phenylindole (DAPI). Retina wholemounts and cryosections were mounted with Fluoromount-G mounting medium. Photoreceptor cell count was performed as previously described [10, 18]. The thickness of the outer nuclear layer (ONL) and inner nuclear layer (INL) was quantitated with the Thickness

Tool [19]. Slides were imaged with or ZEISS (Thornwood, NY) LSM 800 laser confocal microscope or ZEISS Axio epifluorescence microscope. Fluorescence (integrated density) was quantitated in 8-bit digital images using ImageJ (version 1.52, http://imagej.nih.gov/ij/; provided in the public domain by the National Institutes of Health, Bethesda, MD).

Flow Cytometry Analyses

Retinas were isolated following RD and processed using the Papain Dissociation System (Worthington, Columbus, OH) into a single-cell suspension, according to the manufacturer's instructions. For flow cytometry analysis, we used Zombie NIR live/dead exclusion assay from BioLegend (San Diego, CA) and DAPI staining to detect nucleated live singlets. Antibodies were purchased from BioLegend (CD11b) and BD Biosciences (CD45, Ly6G, and Ly6C). Fluorescence-minus-one, unstained, and singlestain controls were used to compensate settings for each antibody or fluorescent reporter. Gating was performed as previously described [1, 16]. Samples were acquired with Aurora Spectral Cytometer (Cytek Biosciences, Fremont, CA) and data was analyzed with Kaluza cytometry software (Beckman Coulter, Brea, CA).

Statistical Analyses

Statistical analyses were performed with SAS Software (2016, SAS Institute Inc., Cary, NC). The Shapiro–Wilk test was used to check for normality. Statistical significance for differences between groups was determined with a two-sided T-test or Student's T-test for two-group comparisons. Results are expressed as mean ± standard error of the mean (SEM). A p-value of 0.05 or less was deemed to indicate statistical significance.

Results

Recent Use of Transvitreal and Transscleral Models of RD

We performed a literature search to investigate the usage of RD models over the past decades. We identified a steady increase in the use of this experimental model from 2003 to 2023 (Fig. 1C), with 24 references using the TV model and 39 the TS model. The TV model was more frequently used between 2003–2011 (TV = 14, TS = 9), while the TS succeeded and became the most predominant model between 2012–2023 (TV = 10, TS = 30) (Fig. 1D). These results suggest that the TS model is currently the most widely used preclinical RD model.

Transscleral RD Model Induces Higher CCR2^{+} Infiltration in Early RD

We hypothesized that the different approaches to induce an RD in the TV and TS models could trigger a differential expression of inflammatory markers and leukocyte recruitment. To determine the early expression of these markers in the detached retina, we induced an RD in CX3CR1$^{+/GFP}$ CCR2$^{+/RFP}$ mice and quantitated the number of CD11b^{+}, CX3CR1^{+}, and CCR2^{+} cells in the detached retina (Fig. 2A-H). We observed that the number of total CD11b^{+} and CD11b^{+} CX3CR1^{+} cells in the TS model was higher than in the TV model at day one post-RD, yet not statistically significant ($p = 0.104$ and 0.252, respectively) (Fig. 2I). In contrast, the number of CD11b^{+} CCR2^{+} cells increased over threefold in the TS model, significantly higher than in the TV model

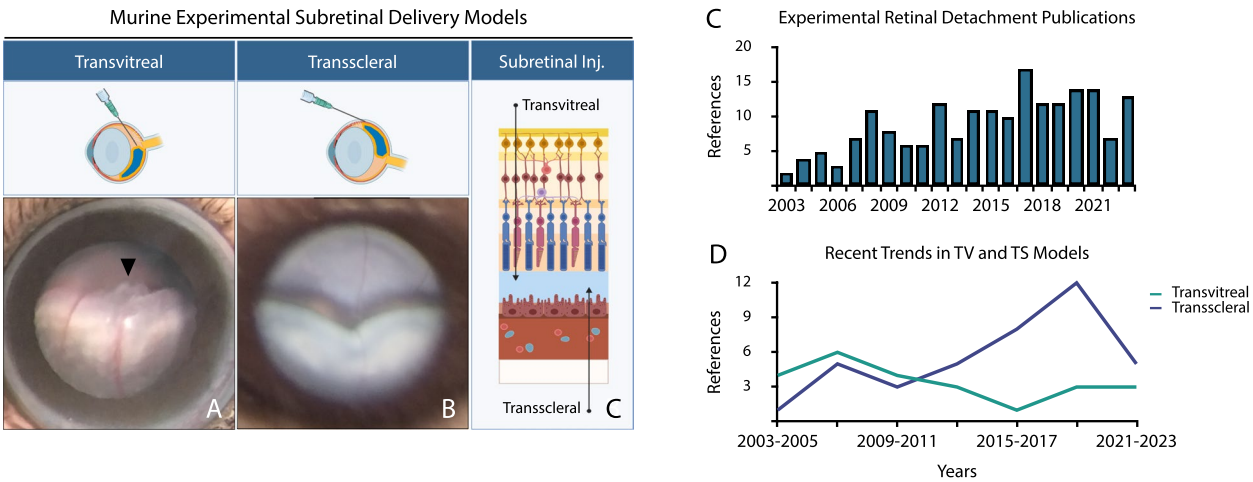

Fig. 1 Outline of Transvitreal and Transscleral Experimental Retinal Detachment (RD) Models. **A** Outline and fundus image of transvitreal RD model displaying bullous detachment and retinotomy at the injection site (arrowhead). **B** Outline and fundus image of transscleral RD model showing bullous detachment without retinal tears/holes. (**A**-**B**) Created with BioRender.com. **C** Experimental retinal detachment publications from 2003 to 2023. **D** References using transvitreal and transscleral models from 2003 to 2023

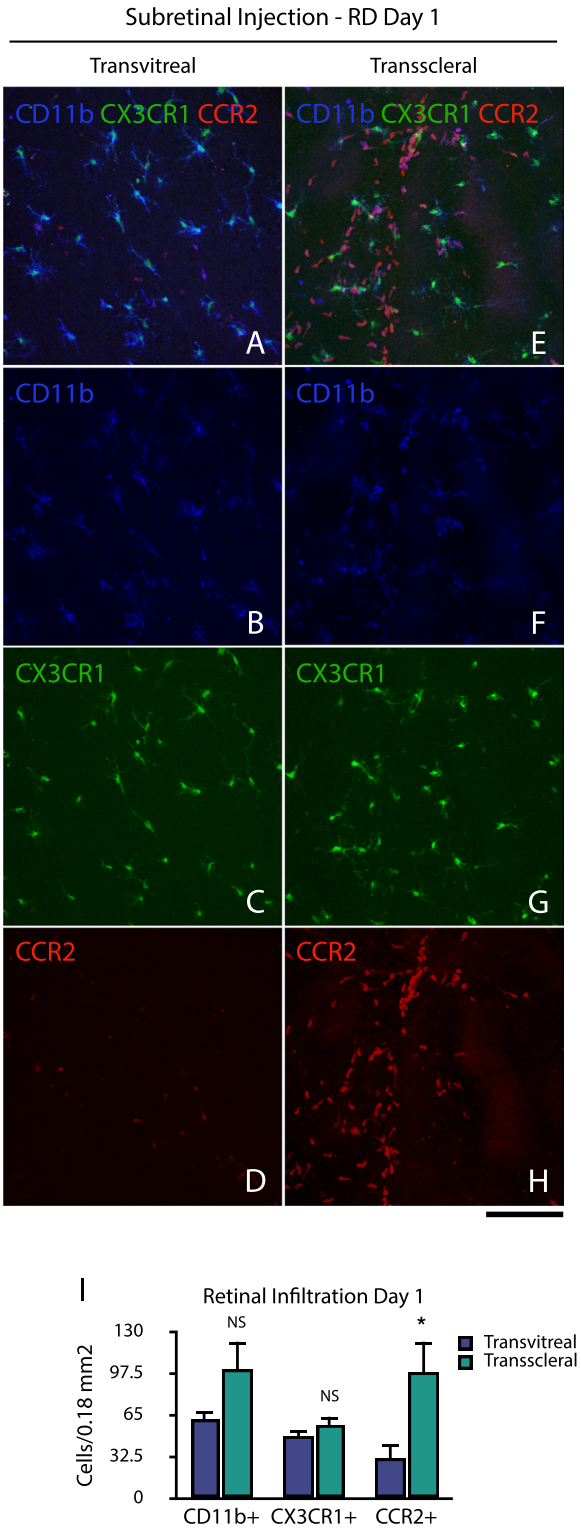

◀ **Fig. 2** Differences in Early Retinal Infiltration after Retinal Detachment (RD) in CX3CR1$^{+/GFP}$ CCR2$^{+/RFP}$ mice. Retinal infiltration of total CD11b^{+}, CD11b^{+} CX3CR1^{+}, and CD11b^{+} CCR2^{+} cells in the (**A**-**D**) Transvitreal and (**E**–**H**) Transscleral RD models. Scale bar 50 µm (**A**-**H**). (**I**) Quantitation of CD11b+, CX3CR1+, and CCR2+cells in the detached retina in retinal wholemounts ($n=3$). *$=p<0.05$; NS = not significant

(99.17 ± 24.34 vs. 30.57 ± 11.33 cells, $p=0.021$). These results indicate that the TS model has an early predominance of CD11b^{+} CCR2^{+} inflammatory cells, likely derived from peripheral leukocytes.

Divergence in Ly6G^{+} and Ly6C^{+} Early Infiltration in Transvitreal and Transscleral RD Models

Given the early infiltration of the detached retina in these models, we immunophenotyped the infiltrating leukocytes using flow cytometry (Fig. 3A-D). We observed that the TS model had a significantly higher proportion of CD45^{hi} CD11b^{+} macrophage/microglia-like cells ($p=0.010$) and CD45^{hi} CD11b^{+} Ly6G^{+} neutrophils ($p=0.017$) than the TV model. In contrast, there was a significantly higher proportion of CD45^{hi} CD11b^{+} Ly6G^{-} Ly6C^{+} monocytes in the TV model ($p=0.048$) compared to the TS model. These results suggest that in early RD, the TV and TS model diverge in their Ly6G^{+} neutrophil and Ly6C^{+} monocyte infiltration.

Transscleral RD Induces Higher Photoreceptor Cell Death in Late RD

Considering the divergence in retinal leukocyte infiltration, we hypothesized that such an inflammatory burden could translate into different photoreceptor cell death in late RD. For this purpose, we analyzed the photoreceptor survival at day seven following RD, as previously described (Fig. 4A-G) [10]. Using Nrl-EGFP^{+} mice, which specifically labels rod photoreceptors, we found that transscleral delivery resulted in a reduced number of rods and segments seven days after retinal detachment. We observed that the number of photoreceptors in the detached retina was significantly lower in the TS model compared to the TV model (1067.41 ± 32.49 vs. 920.58 ± 34.40 photoreceptors, $p=0.019$), which indicates a higher cell death rate in the TS model. The normalized photoreceptor survival rate (detached/attached count) was 63.85 ± 1.76% for the TV model and 48.80 ± 2.79% for the TS model ($p<0.004$). Similarly, the ONL/INL ratio of the detached retina was lower in the TS model (1.16 ± 0.20) than in the TV model (1.22 ± 0.20), yet not significantly ($p=0.542$). Similarly, the increased photoreceptor death in the TS model was paralleled by higher subretinal infiltration of CD11b^{+} cells (12.31 ± 1.76 cells)

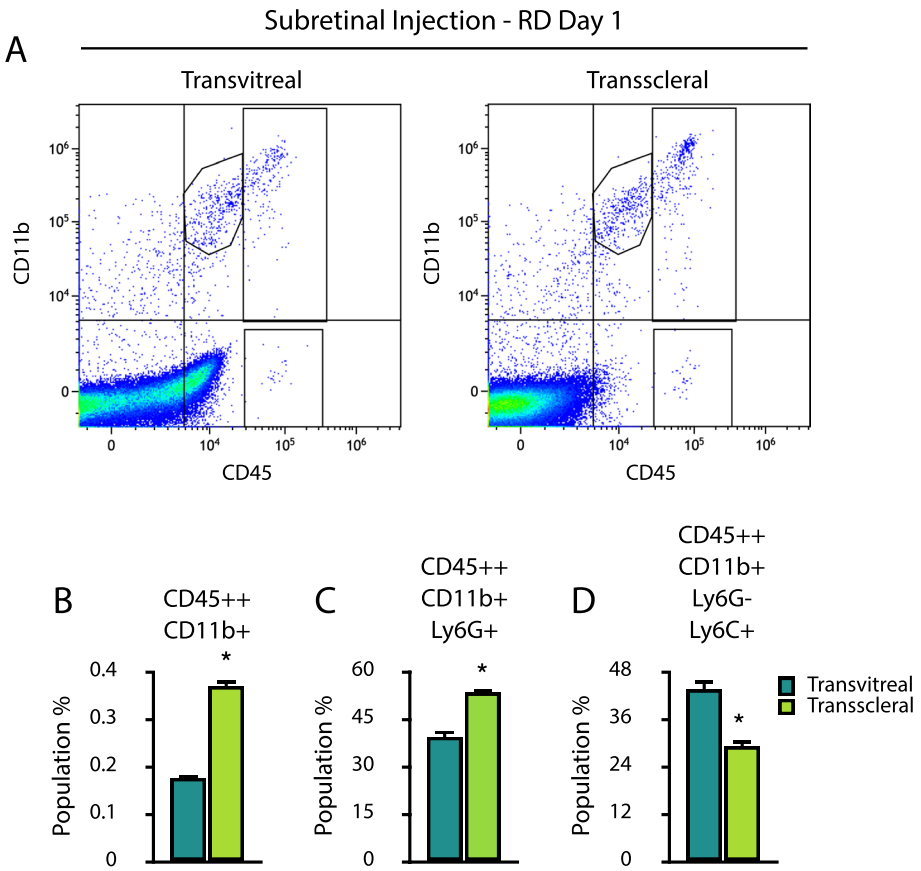

Fig. 3 Immunophenotype of Early Retinal Infiltration in Retinal Detachment (RD) Models. **A** Flow cytometry analyses of retinal single-cell suspension isolated form the detached retina at day 1 after RD in transvitreal and transscleral models. Quantitation of (**B**) live $CD45^{hi}$ $CD11b^{+}$ cells, (**C**) $CD45^{hi}$ $CD11b^{+}$ $Ly6G^{+}$, and (**D**) $CD45^{hi}$ $CD11b^{+}$ $Ly6G^{+}$ $Ly6C^{+}$ in the detached retina at day 1 after RD. ($n=6$). *$=p<0.05$

compared to the TV model (11.16 ± 1.16 cells), yet not statistically significant ($p=0.614$).

Transvitreal and Transscleral RD Models Induce Significant Reactive Gliosis

Considering the tapping into the retinal tissue required for the TV model and the higher cell death observed in the TS model, we sought to investigate the wound healing response in the detached retina in late RD. For this purpose, we quantitated retinal gliosis by glial fibrillary acidic protein (GFAP) fluorescence (integrated density) in retinal cryosections and whole-mounts on day seven following RD (Fig. 5A-G). We found that both the TV and TS models had a significant gliotic reaction in the detached retina compared to the attached region (TV, $p<0.001$; TS, $p=0.026$) (Fig. 5G). We found no differences between the TV and TS models in the attached ($p=0.146$) or detached retina ($p=0.698$). These results suggest that the higher cell death in the TS model and higher expected gliotic response for this model might be compensated by the direct retinal tapping in the TV model, given comparable late GFAP intensities in these models.

Discussion

In this work, we showed that the TS injection caused higher $CD45^{++}$ $CD11b^{+}$, $CD11b^{+}$ $CCR2^{+}$, and $Ly6G^{+}$ leukocyte infiltration of the retina, while the TV model was associated with higher $Ly6C^{+}$ cell infiltration in early phases. Moreover, we observed that the TS subretinal approach caused higher photoreceptor cell death than the TV model. These results indicate the divergence in immune response and different photoreceptor demise between the two subretinal delivery approaches.

The TS model has been the predominant subretinal delivery approach for RD during the period of 2012–2014. In 2013, Matsumoto et al. described in 2013 a technical modification to the TS model, using surgical adhesives to seal the sclerotomy [3]. This modification reduced sodium hyaluronate leakage and subsequent retinal detachments in a reproducible manner, in both height and duration, and resulted in lower retinal/choroidal hemorrhage rates. We speculate that this

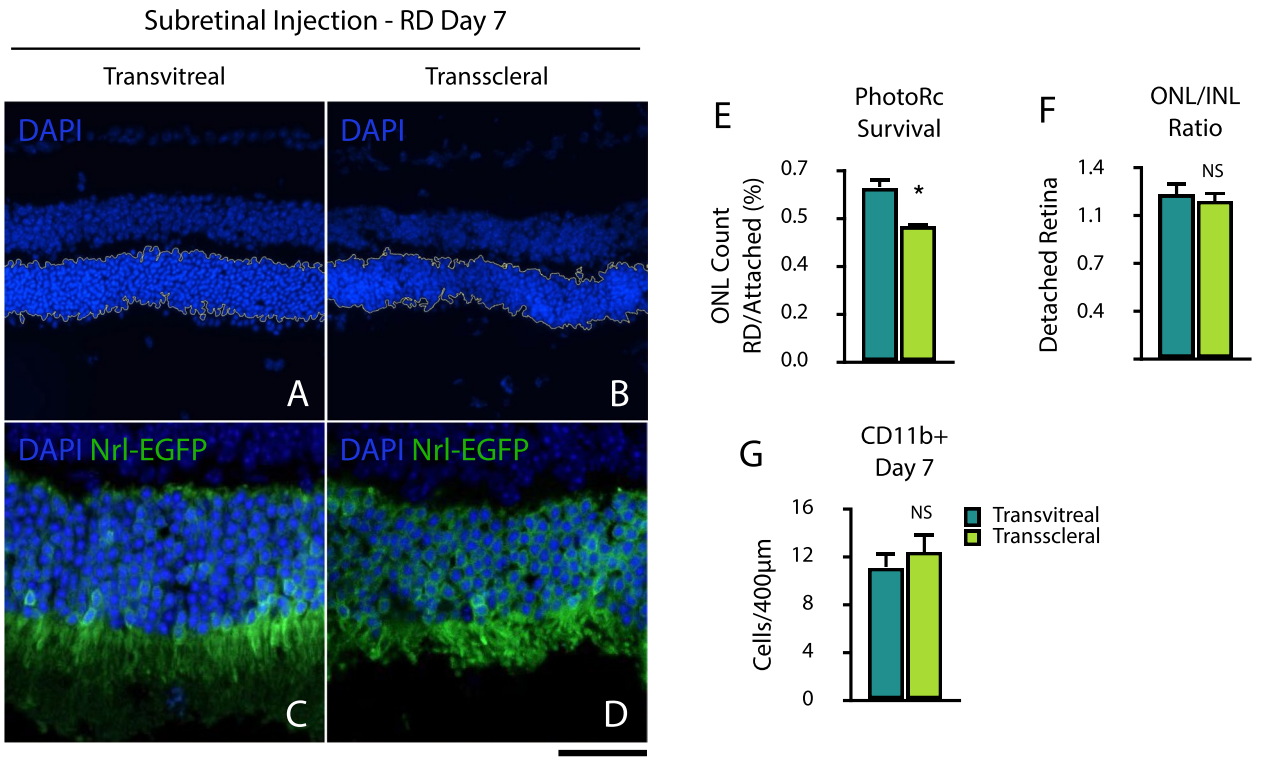

Fig. 4 Late Photoreceptor Survival and Subretinal Space Infiltration in Transvitreal and Transscleral Models. **A**-**B** Representative retinal cryosection images of detached retinas outlining the outer nuclear layer region of interest (yellow line). (**C**-**D**) Representative cryosection images of retinal detachment in Nrl-EGFP animals showing fewer rods with shorter segments. (**C**-**D**) Scale bar 100 µm (**A**-**B**) and 40 µm (**C**-**D**). Quantitation of (**C**) photoreceptor cell count, (**D**) ONL/INL ratio, and (**E**) subretinal space infiltration of $CD11b^+$ cells ($n = 4–6$). * = $p < 0.05$; NS = not significant; PhotoRc = photoreceptor; ONL = outer nuclear layer; INL = inner nuclear layer

modification facilitated the study of late RD phases by providing a more reproducible RD model and by giving an edge over the technically complex TV model.

Preclinical adaptation of this subretinal injection RD model in rodents has enabled research by improving cost-effectiveness, reliability, and reproducibility of animal experiments, while allowing genetic manipulations for gain- or loss-of-function studies [20]. Despite their widespread applicability, both TV and TS approaches have limitations that need consideration. For example, the TV approach requires inserting a needle or cannula through the vitreous under direct retina visualization. At the entry site (nasal sclerotomy), there is a local outer blood-retinal-barrier (BRB) disruption and likely inner BRB disturbance due to the retinotomy created to access the vitreous cavity. At the temporal retina, tapping into the retina and creating a retinotomy to access the SRS induces physical trauma and likely affects the inner BRB. Besides the possibility of vitreous, preretinal, intraretinal, subretinal, or sub-RPE hemorrhages, this approach may carry risks associated with vitreous humor manipulation, such as traumatic cataracts. Leon et al. have shown that puncture of the lens can induce macrophage infiltration of the retina in an optic nerve crush model [21]. In addition, the persistence of a retinotomy allows vitreous contents to seep through this gap and enter the subretinal space, as observed in rhegmatogenous RD. The TS subretinal injection provides access to the SRS and suprachoroidal space without entering the vitreous cavity or tapping into the retina. Compared to the TV model, there is only a local disruption of the outer BRB at the entry site (temporal sclerotomy). Such differences in BRB disruption between these approaches may affect the subsequent inflammatory response [22]. Inasmuch, the clinical applications for this approach are promising, as dedicated microinjectors are being developed for a reproducible and safer TS suprachoroidal injection [23].

Previous work in rodents showed that photoreceptor cell death following RD peaks at day 1, with approximately 25% of total photoreceptors lost in that period [10, 24]. Clinical trials for gene therapy have injected volumes of 150 to 300 µL to the SRS [25, 26]. Despite prompt reabsorption [25], the subretinal injection of 100 µL of balanced salt solution in the macular region of cynomolgus macaques has been associated with mfERG suppression in retinal areas corresponding to the bleb but

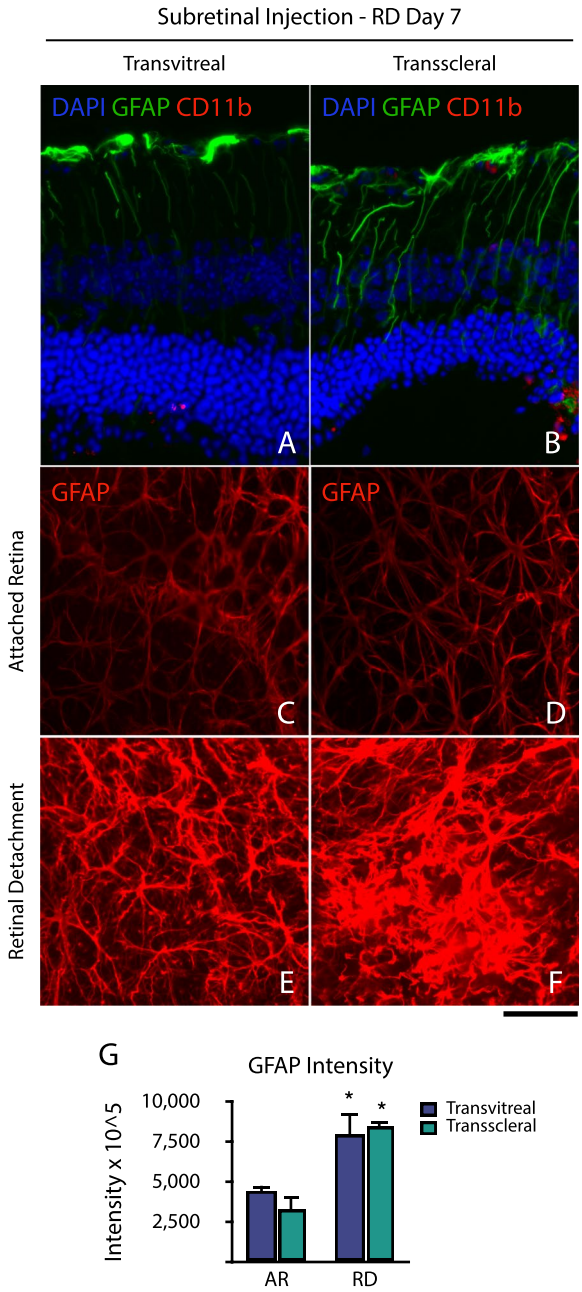

Fig. 5 Late Gliotic Changes in Transvitreal and Transscleral Retinal Detachment (RD) Models. **A**-**B** Representative cryosection images of retinal detachment on day 7. **C**-**F** Representative wholemount confocal images of glial fibrillary acidic protein (GFAP) intensity in the attached and detached retina. Scale bar 70 µm (**A**-**B**) and 100 µm (**C**-**F**). (**G**) Quantitation of GFAP fluorescence intensity in transvitreal and transscleral RD models at day 7 ($n=4$). $*=p<0.05$

also adjacent to this site [5]. Despite recovery of mfERG amplitudes after 90 days, authors describe decreased reflectivity of the photoreceptor inner segment/outer segment line in SD-OCT and histological retinal disorganization in transmission electron microscopy. These findings suggest that the impact of subretinal injections and localized retinal detachment on photoreceptor structure and function is worth considering.

Regarding the inflammatory response, subretinal injection of phosphate-buffered saline using the TS approach in *rd10* mice showed overexpression of CCL2 and CCL12 in the retina and RPE/choroid compared to wild-type mice [2]. These exaggerated cytokine responses suggest the different burden of these injections in retinas with preexisting photoreceptor degeneration. Previous work from our group showed that peripheral neutrophils and monocytes contribute to photoreceptor cell death in RD [16]. Using the TS approach, the depletion of neutrophils and monocytes protected the outer retina. This detrimental role of peripheral monocytes could be even more relevant in the TV model since this approach had higher infiltration of Ly6C + cells than the TS model.

Our work has several limitations. First, there are technical differences between these subretinal injection approaches, such as: i) tapping into the retinal surface; ii) injection of viscoelastic materials; iii) corneal paracentesis; and iv) use of surgical adhesives. First, the touchdown of the injector on the retina has been linked to areas of early chorioretinal atrophy following subretinal delivery of voretigene neparvovec-rzyl [4]. In our work, we used a 34-gauge injector to access the subretinal space through the retina. Several authors use different injectors with different needle gauges, from 34-35G [1, 2] to an 80G [27] glass injector. Given the lower gauge of our injector, we observe the retinotomy in the retinal surface in the TV model, which suggests a higher degree of retinal injury or sodium hyaluronate leakage into the vitreous cavity. However, photoreceptor cell death was lower in the TV model, and the retinal detachment had a similar aspect and height at seven days post-RD compared to the TS model. These findings suggest that the impact of the retinotomy on local photoreceptor cell death may not be as high as anticipated and that leakage of the viscoelastic material into the vitreous would be minimal, if any. Second, since hyaluronic acid is the predominant glycosaminoglycan in the human vitreous [28], different concentrations of sodium hyaluronate have been delivered to the subretinal space to create an RD. In this work, we used sodium hyaluronate 1%, while different research groups have used solutions from 1% [1, 16, 29] (Provisc®, Alcon) to 1.4% [7, 27, 30, 31] (Healon GV®, Alcon) sodium hyaluronate. However, results obtained with these viscoelastic materials may not necessarily parallel those observed with solutions delivered in clinical trials since even solution osmolarity can affect subretinal bleb resorption [32]. Third, a corneal paracentesis is created in the TS model to avoid increased intraocular pressure while injecting sodium hyaluronate. Such pressure

increase would lead to leakage of this viscoelastic material from the sclerotomy and, ultimately, a shallow RD. In the TV model, the initial sclerotomy accesses the vitreous cavity and allows liquified vitreous to egress from the eye. This prevents an increase in intraocular pressure while injecting sodium hyaluronate. However, the effects of corneal paracentesis should not be overlooked. Lambiase and colleagues showed that a corneal paracentesis, used as a sham control for surgical iridectomy in rabbits, increased the concentration of nerve growth factor (NGF) in the aqueous humor after four hours and remained elevated at four days compared to baseline [33]. Interestingly, endogenous NGF, likely secreted by retinal microglia, has been linked to increased neuronal cell death during development in the chick retina and in the cultured 661w murine photoreceptor cell line [34–36]. Likewise, Chen et al., demonstrated that a penetrating injury to the cornea results in rapid infiltration of bone marrow-derived $CX3CR1^{+}$ monocytes into the retina with subsequent neuroretinal cell death as a result of TNF-α, IL-1β, and IL-6 cytokine upregulation in the retina [37]. The reported severity of retinal damage was shown to be proportional to the degree of ocular injury. We speculate that this mechanism could contribute to the higher photoreceptor cell death observed in the TS model. Finally, wound closure is critical to avoid sclerotomy leakage in TS approaches. Cyanoacrylate-based surgical adhesives have been used to manage corneal wounds in clinical practice and veterinary medicine [38, 39]. Ollivier et al. showed that these adhesives caused minimal inflammation when sealing a corneal defect while not interfering with the wound healing response [38]. However, it is worth mentioning that cyanoacrylate has been associated with corneal neovascularization after one month [40], suggesting that the impact of such adhesives on inflammation and angiogenesis is not negligible.

In summary, this work demonstrates that TV and TS approaches are instrumental for subretinal delivery. Divergence in immune response and different cell death kinetics should be considered when designing neuroprotective or regenerative strategies. Tailored subretinal approaches for selected retinal degenerative diseases can improve the outcomes of such therapies.

Supplementary Information

The online version contains supplementary material available at https://doi.org/10.1186/s12950-025-00433-1.

Supplementary Material 1.

Literature Search

A literature search to investigate the retinal detachment models in mice over the past 20 years was conducted. The terms were "retinal detachment" and "mouse" were searched in a public database (Pubmed). References published between January 1, 2003, and November 30, 2023, were included. Form 192 references, 125 were excluded due to lack of experimental data or unclear methodology for subretinal injections. A total of 67 references with detailed methods describing TV or TS approaches were included for further analysis.

Authors' contributions

Author contributions: DEM and DGV designed research. DEM performed the experiments, analyzed the data, and drafted the manuscript. SPP assisted in performing the experiments and analyzing the data. CW and SC performed the literature search. LGB, EIP, AK, and DGV reviewed the data and made substantial intellectual contributions to the research design and manuscript. All authors reviewed the manuscript.

Funding

This work was supported by funding from the National Institutes of Health K08EY034935 (DEM), Research to Prevent Blindness Career Development Award (DEM), UIC K12 Independent Clinical Vision Scientist Development Program K12EY021475 (DEM), Alfonso Martin Escudero Foundation (LGB), NEI R21EY023079-01 A1 and R01EY02536201 (DGV), Yeatts Family foundation (DGV), Martin S Loeffler Renewed Hope Foundation (DGV), ARI Young Investigator Award (DGV), RPB Physician-Scientist Award (DGV), NEI P30EY001792 Core Grant (UIC), Research to Prevent Blindness Unrestricted Departmental Grant (UIC), and P30EY014104 (MEEI). The funders had no role in study design, data collection and analysis, decision to publish or preparation of the manuscript.

Financial Disclosure

The authors have no relevant financial relationships or interests to disclose.

Data availability

The data that support the findings of this study will be openly available in the Open Science Framework from the Center for Open Science at https://osf.io/yztn3. Ethics Statements The Animal Care Committee of the University of Illinois Chicago reviewed and approved all animal protocols.

Declarations

Ethics approval and consent to participate

The animals used for experiments and breeding strictly followed the guidelines set forth by the Association for Research in Vision and Ophthalmology (ARVO). The Animal Care Committee of the University of Illinois Chicago reviewed and approved all animal protocols.

Competing interests

The authors declare no competing interests.

Received: 18 April 2024 Accepted: 28 January 2025
Published online: 07 February 2025

References

1. Kiang L, Ross BX, Yao J, Shanmugam S, Andrews CA, Hansen S, et al. Vitreous Cytokine Expression and a Murine Model Suggest a Key Role of Microglia in the Inflammatory Response to Retinal Detachment. Invest Ophthalmol Vis Sci. 2018;59:3767.
2. Maidana DE, Gonzalez-Buendia L, Miller JW, Vavvas DG. RIPK necrotic cell death pathway in both donor photoreceptor and host immune cells synergize to affect photoreceptor graft survival. FASEB J. 2023;37:e22847.
3. Matsumoto H, Miller JW, Vavvas DG. Retinal detachment model in rodents by subretinal injection of sodium hyaluronate. J Vis Exp. 2013;79:50660.
4. Gange WS, Sisk RA, Besirli CG, Lee TC, Havunjian M, Schwartz H, et al. Perifoveal Chorioretinal Atrophy after Subretinal Voretigene Neparvovec-rzyl for RPE65-Mediated Leber Congenital Amaurosis. Ophthalmology Retina. 2022;6:58–64.
5. Nork TM. Functional and Anatomic Consequences of Subretinal Dosing in the Cynomolgus Macaque. Arch Ophthalmol. 2012;130:65.

6. Zacks DN, Ha¨nninen V, Pantcheva M, Ezra E, Grosskreutz C, Miller JW. Caspase Activation in an Experimental Model of Retinal Detachment. Invest Ophthalmol Vis Sci. 2003;44:1262.
7. Yang L, Bula D, Arroyo JG, Chen DF. Preventing Retinal Detachment-Associated Photoreceptor Cell Loss in Bax-Deficient Mice. Invest Ophthalmol Vis Sci. 2004;45:648.
8. Zacks DN, Zheng Q-D, Han Y, Bakhru R, Miller JW. FAS-Mediated Apoptosis and Its Relation to Intrinsic Pathway Activation in an Experimental Model of Retinal Detachment. Invest Ophthalmol Vis Sci. 2004;45:4563.
9. Trichonas G, Murakami Y, Thanos A, Morizane Y, Kayama M, Debouck CM, et al. Receptor interacting protein kinases mediate retinal detachment-induced photoreceptor necrosis and compensate for inhibition of apoptosis. Proc Natl Acad Sci. 2010;107:21695–700.
10. Maidana DE, Gonzalez-Buendia L, Miller JW, Vavvas DG. Local photoreceptor cell death differences in the murine model of retinal detachment. Sci Rep. 2021;11:18798.
11. Matsumoto H, Murakami Y, Kataoka K, Lin H, Connor KM, Miller JW, et al. Mammalian STE20-like kinase 2, not kinase 1, mediates photoreceptor cell death during retinal detachment. Cell Death Dis. 2014;5:e1269–e1269.
12. Kataoka K, Matsumoto H, Kaneko H, Notomi S, Takeuchi K, Sweigard JH, et al. Macrophage- and RIP3-dependent inflammasome activation exacerbates retinal detachment-induced photoreceptor cell death. Cell Death Dis. 2015;6:e1731.
13. Sweigard JH, Matsumoto H, Smith KE, Kim LA, Paschalis EI, Okonuki Y, et al. Inhibition of the alternative complement pathway preserves photoreceptors after retinal injury. Sci Transl Med. 2015;7:297ra116.
14. Wang X, Miller EB, Goswami M, Zhang P, Ronning KE, Karlen SJ, et al. Rapid monocyte infiltration following retinal detachment is dependent on non-canonical IL6 signaling through gp130. J Neuroinflammation. 2017;14:121.
15. Okunuki Y, Mukai R, Pearsall EA, Klokman G, Husain D, Park D-H, et al. Microglia inhibit photoreceptor cell death and regulate immune cell infiltration in response to retinal detachment. Proc Natl Acad Sci USA. 2018;115:E6264–73.
16. Maidana DE, Gonzalez-Buendia L, Pastor-Puente S, Naqvi A, Paschalis E, Kazlauskas A, et al. Peripheral monocytes and neutrophils promote photoreceptor cell death in an experimental retinal detachment model. Cell Death Dis. 2023;14:834.
17. Ladha R, Caspers LE, Willermain F, De Smet MD. Subretinal Therapy: Technological Solutions to Surgical and Immunological Challenges. Front Med. 2022;9:846782.
18. Byun J, Verardo MR, Sumengen B, Lewis GP, Manjunath BS, Fisher SK. Automated tool for the detection of cell nuclei in digital microscopic images: application to retinal images. Mol Vis. 2006;12:949–60.
19. Maidana DE, Notomi S, Ueta T, Zhou T, Joseph D, Kosmidou C, et al. ThicknessTool: automated ImageJ retinal layer thickness and profile in digital images. Sci Rep. 2020;10:18459.
20. Vandamme TF. Use of rodents as models of human diseases. J Pharm Bioallied Sci. 2014;6:2–9.
21. Leon S, Yin Y, Nguyen J, Irwin N, Benowitz LI. Lens Injury Stimulates Axon Regeneration in the Mature Rat Optic Nerve. J Neurosci. 2000;20:4615–26.
22. Yiu G, Chung SH, Mollhoff IN, Nguyen UT, Thomasy SM, Yoo J, et al. Suprachoroidal and Subretinal Injections of AAV Using Transscleral Microneedles for Retinal Gene Delivery in Nonhuman Primates. Molecular Therapy - Methods & Clinical Development. 2020;16:179–91.
23. Hejri A, Bowland II, Nickerson JM, Prausnitz MR. Suprachoroidal Delivery in Rats and Guinea Pigs Using a High-Precision Microneedle Injector. Trans Vis Sci Tech. 2023;12:31.
24. Matsumoto H, Kataoka K, Tsoka P, Connor KM, Miller JW, Vavvas DG. Strain Difference in Photoreceptor Cell Death After Retinal Detachment in Mice. Invest Ophthalmol Vis Sci. 2014;55:4165.
25. Maguire AM, Simonelli F, Pierce EA, Pugh EN, Mingozzi F, Bennicelli J, et al. Safety and Efficacy of Gene Transfer for Leber's Congenital Amaurosis. N Engl J Med. 2008;358:2240–8.
26. Gao J, Hussain RM, Weng CY. Voretigene Neparvovec in Retinal Diseases: A Review of the Current Clinical Evidence. OPTH. 2020;14:3855–69.
27. Conart J-B, Blot G, Augustin S, Millet-Puel G, Roubeix C, Beguier F, et al. Insulin inhibits inflammation-induced cone death in retinal detachment. J Neuroinflammation. 2020;17:358.
28. Schwartz DM, Shuster S, Jumper MD, Chang A, Stern R. Human vitreous hyaluronidase: isolation and characterization. Curr Eye Res. 1996;15:1156–62.
29. Xie J, Zhu R, Peng Y, Gao W, Du J, Zhao L, et al. Tumor necrosis factor-alpha regulates photoreceptor cell autophagy after retinal detachment. Sci Rep. 2017;7:17108.
30. Nakazawa T, Takeda M, Lewis GP, Cho K-S, Jiao J, Wilhelmsson U, et al. Attenuated Glial Reactions and Photoreceptor Degeneration after Retinal Detachment in Mice Deficient in Glial Fibrillary Acidic Protein and Vimentin. Invest Ophthalmol Vis Sci. 2007;48:2760.
31. Yang L, Kim J-H, Kovacs KD, Arroyo JG, Chen DF. Minocycline inhibition of photoreceptor degeneration. Arch Ophthalmol. 2009;127:1475–80.
32. Negi A, Marmor MF. Effects of subretinal and systemic osmolality on the rate of subretinal fluid resorption. Invest Ophthalmol Vis Sci. 1984;25:616–20.
33. Lambiase A, Bonini S, Manni L, Ghinelli E, Tirassa P, Rama P, et al. Intraocular production and release of nerve growth factor after iridectomy. Invest Ophthalmol Vis Sci. 2002;43:2334–40.
34. María Frade J, Rodríguez-Tébar A, Barde Y-A. Induction of cell death by endogenous nerve growth factor through its p75 receptor. Nature. 1996;383:166–8.
35. Frade JM, Barde YA. Microglia-derived nerve growth factor causes cell death in the developing retina. Neuron. 1998;20:35–41.
36. Srinivasan B, Roque CH, Hempstead BL, Al-Ubaidi MR, Roque RS. Microglia-derived Pronerve Growth Factor Promotes Photoreceptor Cell Death via p75 Neurotrophin Receptor. J Biol Chem. 2004;279:41839–45.
37. Chen X, Lei F, Zhou C, Chodosh J, Wang L, Huang Y, et al. Glaucoma after Ocular Surgery or Trauma: The Role of Infiltrating Monocytes and Their Response to Cytokine Inhibitors. Am J Pathol. 2020;190:2056–66.
38. Ollivier F, Delverdier M, Regnier A. Tolerance of the rabbit cornea to an n-butyl-ester cyanoacrylate adhesive (Vetbond ®). Veterinary Ophthalmology. 2001;4:261–6.
39. Sharma A, Kaur R, Kumar S, Gupta P, Pandav S, Patnaik B, et al. Fibrin glue versus N-butyl-2-cyanoacrylate in corneal perforations. Ophthalmology. 2003;110:291–8.
40. Yin J, Singh RB, Al Karmi R, Yung A, Yu M, Dana R. Outcomes of Cyanoacrylate Tissue Adhesive Application in Corneal Thinning and Perforation. Cornea. 2019;38:668–73.

Publisher's Note